DANMARKS OG GRØNLANDS GEOLOGISKE UNDERSØGELSE **RAPPORT 2025/25**

Seismic Data Reprocessing of the DNJ8183D Survey (DNJ8183D-RE2025): Line DNJ-32

Tomi Jusri, Tanni Abramovitz & Lasse M. Rasmussen

GEOLOGICAL SURVEY OF DENMARK AND GREENLAND
DANISH MINISTRY OF CLIMATE, ENERGY AND UTILITIES

G E U S

DANMARKS OG GRØNLANDS GEOLOGISKE UNDERSØGELSE **RAPPORT 2025/25**

Seismic Data Reprocessing of the DNJ8183D Survey (DNJ8183D-RE2025): Line DNJ-32

Technical Report

Tomi Jusri, Tanni Abramovitz & Lasse M. Rasmussen

GEOLOGICAL SURVEY OF DENMARK AND GREENLAND
DANISH MINISTRY OF CLIMATE, ENERGY AND UTILITIES

G E U S

Executive summary

This work focuses on the reprocessing of the legacy seismic profile DNJ-32 from the 2D seismic survey DNJ8183D (DNJ8183D-RE2025), acquired near Aalborg, Denmark, between 1981 and 1983. The goal was to evaluate the feasibility and benefits of applying modern processing workflows to historical seismic data, despite limitations such as missing seismic and navigation information. The reprocessed profile shows improved imaging quality, particularly in resolving thinner geological strata, and demonstrates the potential to extend this approach to other lines within the same survey. The reprocessed seismic profile and the recovered SPS files are available through GEUS's data portal[1].

Key findings

- DNJ-32 was successfully reprocessed, with noticeable improvements in image resolution, allowing for the delineation of thin geological strata that were not visible in the legacy profile.
- The processing workflow applied to DNJ-32 is applicable to other seismic lines in the DNJ8183D survey, assuming similar levels of data availability and quality.
- The geometry setup workflow developed in this work can accelerate geometry configuration for other lines in the same survey.

Limitations

- Some seismic and navigation data could not be recovered, resulting in gaps in the final reprocessed profile.
- The reprocessing workflow was limited to post-stack time migration (POSTM), as the subsurface exhibits a relatively simple geological structure; pre-stack methods were not implemented in this initial phase.
- The overall project timeline was extended by 2–3 weeks due to challenges in reconstructing incomplete seismic and navigation data.

Recommendations for reprocessing other lines in the survey

- Allocate additional time for seismic and navigation data preparation, as historical datasets may require manual correction or interpolation.
- Consider applying pre-stack time migration (PSTM) and pre-stack depth migration (PSDM) to enhance the imaging of fault structures, particularly in geologically complex areas.
- Develop detailed migration velocity models using available well and regional velocity data to improve imaging accuracy and overall image quality.

[1] https://data.geus.dk/ugdata2d3d/procsum.html?proc_id=17604

Table of contents

Table of figures

Figure 18. Close comparison between the legacy profile (left) and the reprocessing result (right). Yellow boxes highlight areas where differences between the two profiles are evident. Yellow arrows indicate high-resolution coherent reflections associated with thinner geological strata, which are not visible in the legacy profile. Blue boxes mark zones where the reprocessing result improves imaging in reflector-free regions of the legacy data. Red arrows point to a fault-like structure in the legacy profile that appears less pronounced in the reprocessing result. Arguably, this feature may also be interpreted as an artifact caused by low fold coverage at the corresponding common mid-point (CMP) location, as it appears perfectly vertical and coincides with a low-fold area indicated by near-surface characteristics of the profile. 28

Tables

1. Introduction

This work was initiated in response to the growing interest in subsurface studies to support future geothermal energy development and Carbon Capture and Storage (CCS) initiatives near Aalborg, Denmark. The Aalborg region has a long history of geological and geophysical investigations, with several seismic surveys have been conducted over the years. One of the most notable is the 2D seismic survey DNJ8183D, acquired by WesternGeco between 1981 and 1983[2] (Figure 1).

One of the key lines from this survey is DNJ-32, a relatively straight profile approximately 63 kilometers in length, running from the northwest to the southeast of the study area. While the legacy profile of DNJ-32 is sufficient for general geological interpretation (Figure 2), both the raw seismic and navigation data are incomplete, and intermediate processing products, such as pre-stack gathers, are unavailable. These limitations are likely common across other lines in the DNJ8183D survey.

This work focuses on reprocessing seismic line DNJ-32 as a test case for the entire DNJ8183D survey. The primary objective is to assess the feasibility of recovering historical seismic datasets and to evaluate the benefits of applying a modern processing workflow to these datasets. As part of the reprocessing, pre-stack gathers were generated, enabling the potential use of advanced techniques, such as pre-stack migration and inversion, in future studies for detailed subsurface characterization.

The reprocessing was completed over approximately eight weeks of effective processing time, spanning from early February to early May 2025. Processing was carried out using GeoThrust (by Geotomo) and Reveal (by Shearwater). This document serves as a technical report on the reprocessing of DNJ-32, outlining the applied workflow, tools, and key processing parameters, and provides recommendations for future reprocessing of other seismic lines in the DNJ8183D survey.

[2] https://data.geus.dk/ugdata2d3d/procsum.html?proc_id=1623

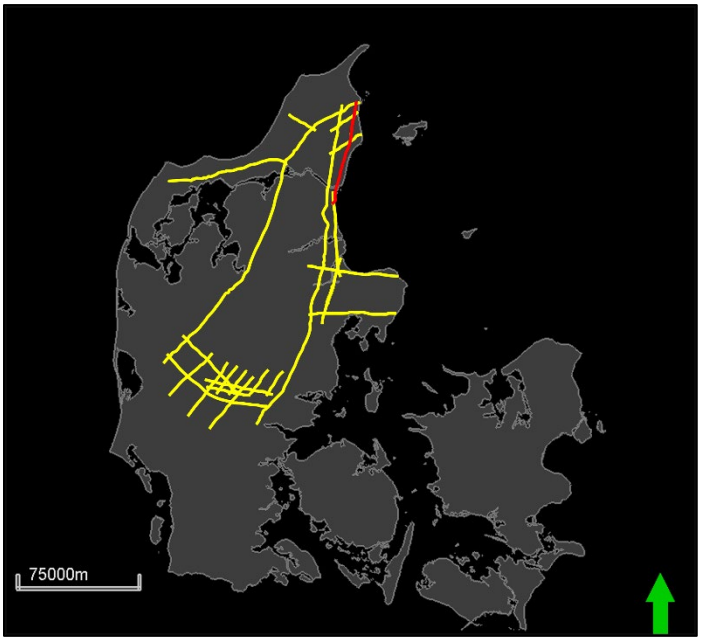

Figure 1. Map showing the location of seismic line DNJ-32 (highlighted in red), acquired as part of the 2D seismic survey DNJ8183D (highlighted in red and yellow). Green arrow indicates north.

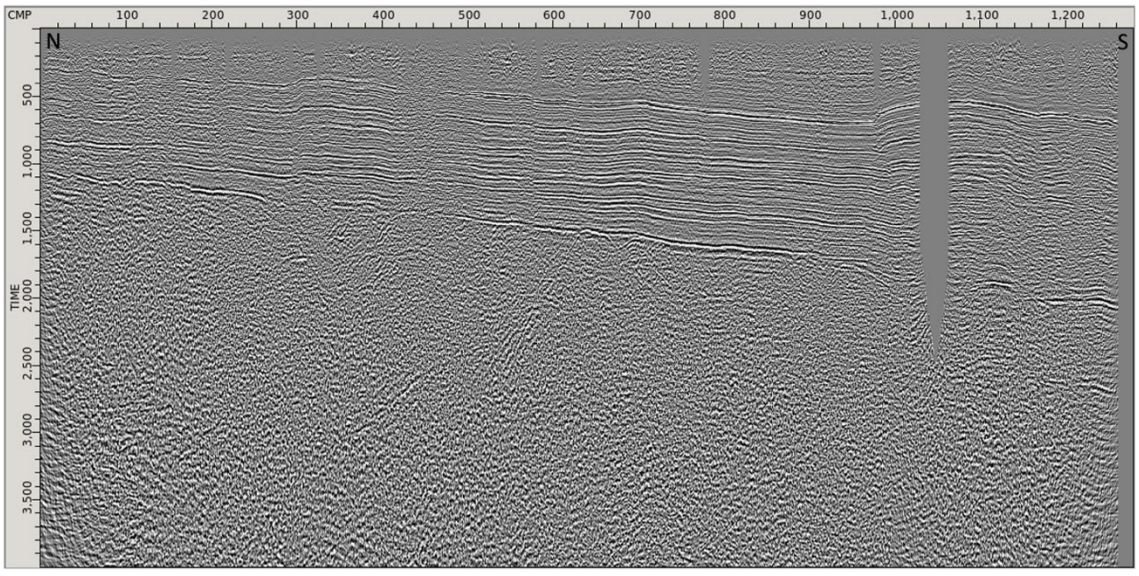

Figure 2. Legacy seismic profile DNJ-32.

2. Processing workflow and parameters

The processing workflow implemented in this project is broadly divided into six main stages:

1. Geometry setup
2. Trace editing
3. Static correction
4. Preprocessing
5. Processing
6. Migration

2.1 Geometry setup

In the geometry setup stage, spatial information from the seismic acquisition was defined in the trace headers and registered in the processing database. This stage included assigning source and receiver coordinates and elevations, as well as determining the active source-receiver relationships.

2.1.1 Navigation data preparation

The navigation data was prepared to generate standard seismic navigation files in Shell Processing Support (SPS) format (commonly referred to as *SPS* files). These files served as input to the seismic processing application for setting up the seismic data geometry. The standard SPS files included:

1. Source file (S-file)—contains source-related information, including:
    - Code
    - Line number
    - Point (station) number
    - Index
    - Depth
    - X and Y coordinates
    - Elevation
2. Receiver file (R-file)—contains the same information as the S-file, but for the receivers. Depth is excluded, as it is not required for the R-file.
3. Cross-reference file (X-file)—defines active source-receiver relationships, including:
    - Code
    - Field File ID (FFID) and FFID increment
    - Shot point line number, station number, and index
    - Active channels and channel increment
    - Receiver line number
    - Recording receiver station
    - Pattern index

The information required to create the SPS files was extracted from the seismic survey navigation data, which was available for reprocessing in the form of:

1. Observer logs
2. Coordinates for each shot and receiver point
3. Elevation and static correction values for each shot and receiver point

Except for the coordinates, the navigation data was received as scanned copies of handwritten documents.

Navigation data preparation was carried out through the following steps:

1. Extracting the following information for each shot and receiver point from the observer logs:
    - Shot and receiver point numbers
    - FFID
    - Active channels
    - Observer comments

The extracted information was entered into a digital *working spreadsheet* for further analysis. Additionally, the observer logs provided information about the planned seismic acquisition layout, as summarized in Table 1.

Table 1. Seismic data acquisition layout.

Line direction	North to South
Spread type	Split-spread roll-along
Maximum number of active channels	48
Receiver interval	100 meters
Near offset	100 meters
Maximum far offset	2400 meters

2. Quality control of the extracted observer log information

    Due to the poor quality of the scanned handwritten documents, many entries were difficult or impossible to read. In such cases, the unclear entries were interpreted based on the planned seismic acquisition layout, as presented in Table 1.

3. Removing redundant shots at the same shot point

    Multiple shots with different FFIDs at the same shot point could have caused issues during geometry setup, as they introduced ambiguity in source positioning and inconsistencies in source-receiver relationships. Redundant shots were identified through visual inspection of raw seismic data. Only the shot gathers with a relatively better signal-to-noise ratio were kept for further processing, and the FFIDs of the redundant shots were removed from the working spreadsheet. In some cases, the differences were minimal, making the selection process subjective.

4. Removing irregular shot records without navigation data

    While the majority of shot records were recorded using a split-spread acquisition layout, a few were acquired with an off-end layout. These irregular shot records also exhibited

much larger near-offsets, resulting in significantly delayed first arrivals compared to the rest of the dataset. Figure 3 shows an example of both regular and irregular shot records.

The navigation data for these irregular shot records could not be recovered from the observer logs due to the poor quality of the scanned handwritten documents, as illustrated in Figure 4. Setting up the geometry for these shot records was not feasible without risking serious errors; therefore, they were excluded from the reprocessing input by removing their corresponding entries from the working spreadsheet.

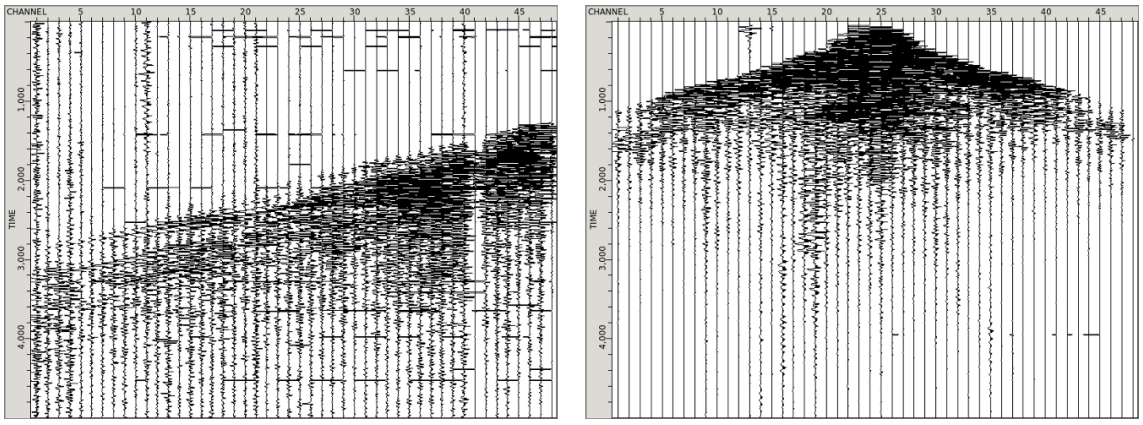

(a) *(b)*

Figure 3. (a) Irregular shot record from an off-end acquisition layout. (b) Regular shot record from a split-spread acquisition layout. Note that the shot in (a) has a much larger near-offset than (b), resulting in significantly delayed first arrivals.

5. Generating SPS files

   SPS files, formatted in ASCII, were generated using the finalized working spreadsheet. These files were then imported into the processing application to create the geometry database.

6. Generating geometry database

   The final step in preparing the navigation data is to generate the geometry database in the processing application. The geometry database compiles information from the SPS files and serves as input for assigning geometry headers, such as source and receiver coordinates, to the raw seismic data.

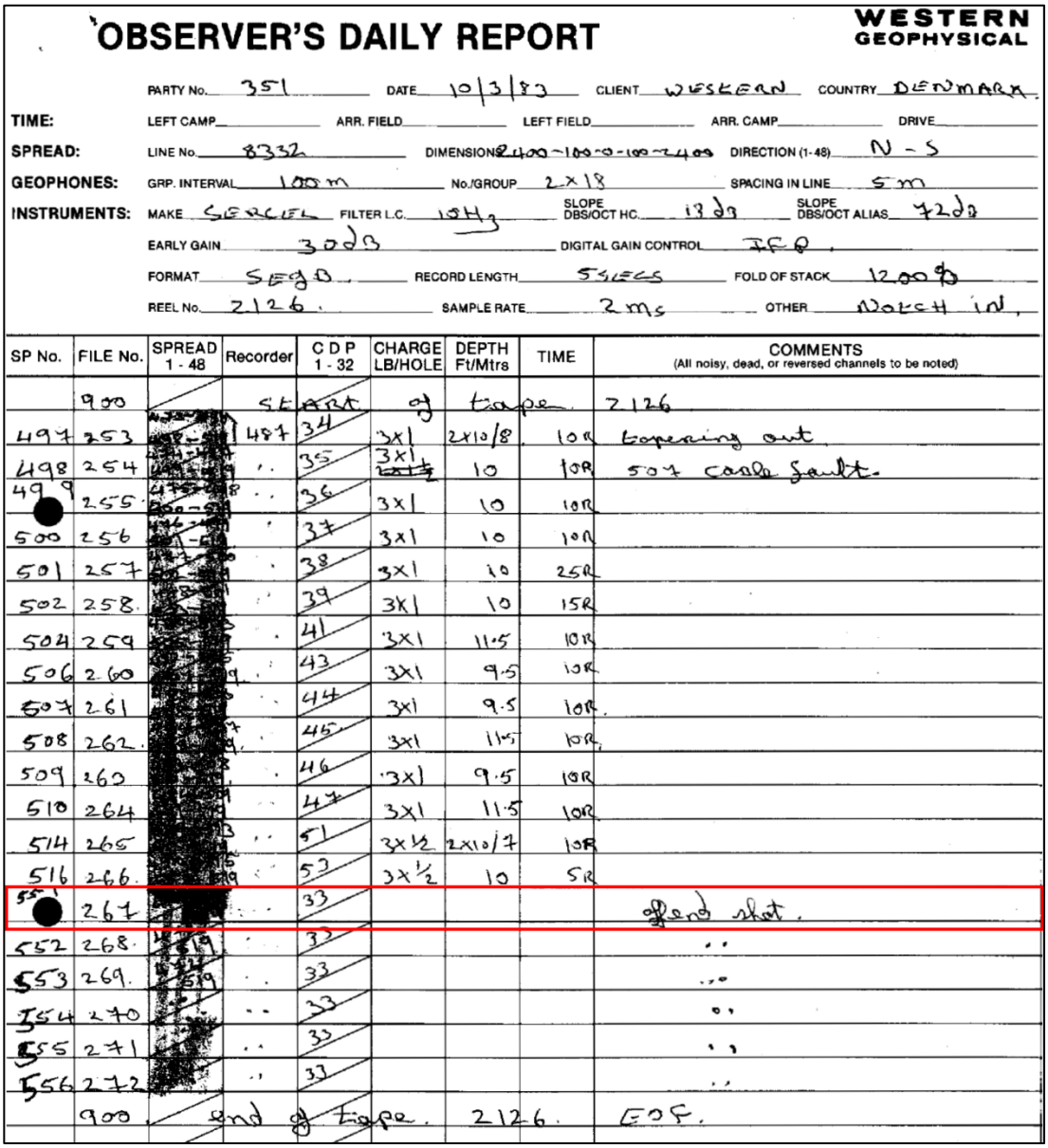

OBSERVER'S DAILY REPORT

WESTERN GEOPHYSICAL

PARTY No. 351 DATE 10/3/83 CLIENT WESTERN COUNTRY DENMARK

TIME: LEFT CAMP ARR. FIELD LEFT FIELD ARR. CAMP DRIVE

SPREAD: LINE No. 8332 DIMENSION 2400-100-0-100-2400 DIRECTION (1-48) N - S

GEOPHONES: GRP. INTERVAL 100 m No./GROUP 2 x 18 SPACING IN LINE 5 m

INSTRUMENTS: MAKE SERCEL FILTER L.C. 10Hz SLOPE DBS/OCT HC. 18 dB SLOPE DBS/OCT ALIAS 72dB

EARLY GAIN 30dB DIGITAL GAIN CONTROL IFP

FORMAT SEGD RECORD LENGTH 5 SECS FOLD OF STACK 12000%

REEL No. 2126 SAMPLE RATE 2 ms OTHER Notch in

SP No.	FILE No.	SPREAD 1 - 48	Recorder	CDP 1 - 32	CHARGE LB/HOLE	DEPTH Ft/Mtrs	TIME	COMMENTS (All noisy, dead, or reversed channels to be noted)
	900			START of tape				2126
497	253		487	34	3x1	2x10/8	10R	tapering out
498	254		"	35	3x1	10	10R	50% cable fault.
499	255		"	36	3x1	10	10R	
500	256		"	37	3x1	10	10R	
501	257		"	38	3x1	10	25R	
502	258		"	39	3x1	10	15R	
504	259		"	41	3x1	11.5	10R	
506	260		"	43	3x1	9.5	10R	
507	261		"	44	3x1	9.5	10R	
508	262		"	45	3x1	11.5	10R	
509	263		"	46	3x1	9.5	10R	
510	264		"	47	3x1	11.5	10R	
514	265		"	51	3x½	2x10/7	10R	
516	266		"	53	3x½	10	5R	
551	267		"	33				dead shot.
552	268		"	33				"
553	269		"	33				"
554	270		"	33				"
555	271		"	33				"
556	272		"	33				"
	900		end	of tape.		2126.		EOF.

Figure 4. Example of an unreadable section from the observer logs. The entry highlighted with a red box corresponds to the shot gather shown in Figure 3a.

1.1.2 Raw seismic data preparation

The raw seismic data for line DNJ-32 was received as shot gathers in SEGY format, with FFIDs and channel numbers stored in the trace headers. Each trace contains 2500 samples at a 2 ms sampling interval, resulting in a 5000 ms record length. No spatial information was present in either the binary or textual headers. The dataset includes 341 shot gathers, comprising dummy shot records, records without navigation data, and records with duplicated FFIDs.

Seismic data preparation was carried out through the following steps:

1. Removing dummy shot records

Dummy shot records are typically generated during recording instrument tests and contain shot records that are irrelevant to processing. Figure 6 shows an example of such records present in the raw seismic data. Dummy shot records were flagged with FFIDs of 900 and above and were excluded from further processing.

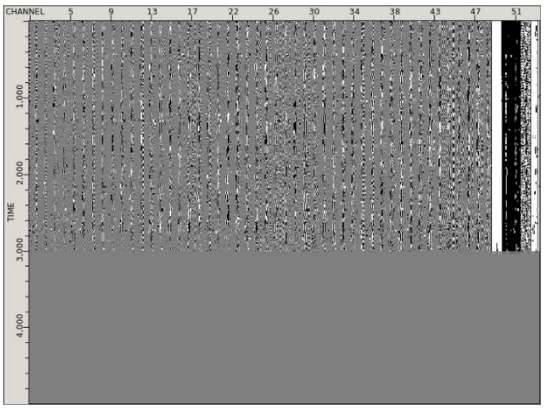

Figure 5. Example of dummy shot records in the raw seismic data.

2. Removing shot records without navigation data

   Shot records lacking navigation data could not be processed and were excluded from further processing.

3. Removing shot records with duplicated FFIDs

   Duplicated FFIDs can cause errors during processing due to ambiguity in source-receiver positioning. These duplicates were identified by plotting FFID against the Trace Sequence Number (TRC) header values from the raw seismic data, as shown in Figure 6a.

   There was no indication in the seismic data headers or navigation data as to which shot records among the duplicates were intended for processing. Therefore, the appropriate records were selected through visual inspection, and only those with a relatively better signal-to-noise ratio were included in the processing workflow. In some cases, the differences were minimal, making the selection process subjective. The plot of FFID versus TRC after removal is shown in Figure 6b, confirming that all remaining FFIDs are unique.

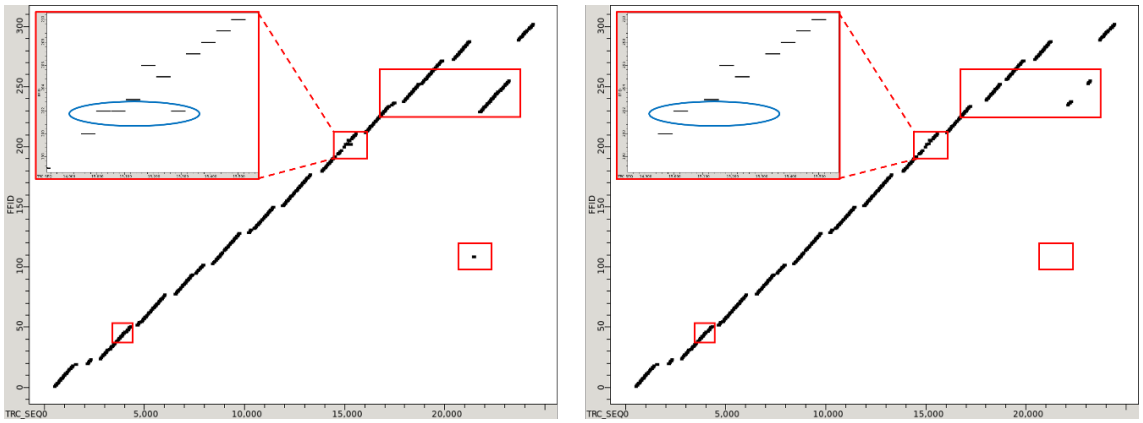

(a) *(b)*

Figure 6. Plot of FFID versus TRC header values. (a) Before removal of duplicated FFIDs. (b) After removal. Red boxes highlight duplicated FFIDs that were present in the raw seismic data but are no longer visible after removal. One red box is exaggerated to more clearly illustrate the removal of two duplicates of FFID 202 as an example.

Furthermore, eight shot records listed in the observer logs were missing from the raw seismic data. In total, 277 out of 341 shot records were included in the processing workflow. Table 2 summarizes the shot record counts considered in the geometry setup.

Table 2. Summary of the shot record counts considered in the geometry setup.

Remark		FFID	Number of shot records	
Raw seismic data (A)				341
Excluded shot records from the processing workflow (B)				64
	Dummy shot records	900-909, 970, 990, 991, 999, 7901, 8311	16	
	One FFID duplicate	46, 109, 229-255	29	
	Two FFID duplicates	202	2	
	Missing navigation data	33, 238	2	
	One shot point duplicate	50, 202, 296	3	
	Irregular shot records	267-272, 283-288	12	
Missing shot records in raw seismic data (C)		113, 178, 179, 193, 198, 199, 201, 204		8
Included shot records in the processing workflow (A - B)				277

1.1.3 Geometry database setup

Geometry setup was performed by assigning spatial information from the geometry database to the raw seismic trace headers. The geometry database and seismic traces were linked using the FFID and active channel numbers present in both datasets. The assigned geometry information included source and receiver coordinates, elevations, point numbers, and source depth. Subsequently, recording offsets and midpoint coordinates were automatically calculated and written to the trace headers. At this stage, the seismic data geometry setup was complete.

2.2 Trace editing

Trace editing was performed to mute unusable shot records (bad shot records) and individual traces (bad traces) caused by corrupted samples or extremely low signal-to-noise ratios. Muted traces were then interpolated using an algorithm based on the anti-leakage Fourier transform. The process was performed sequentially in two data sorts: first in shot sort, then in channel sort.

A despike filter and bandpass filter were applied before scanning for bad shot records and traces. Shot gathers or traces were classified as bad when they could not be recovered using these tools. Table 3 lists the processing tools and parameters used in trace editing. Figure 7 and Figure 8 show examples of bad shot records and bad traces, respectively, before and after interpolation.

Nevertheless, the interpolation algorithm was unable to fill gaps created by an excessive number of consecutively muted shot records, and these gaps remained as muted shot records. Figure 9 shows examples of shot records that could not be interpolated and were therefore left muted. In any case, attempting to interpolate excessively large gaps using inappropriate or overly

aggressive parameters could have introduced processing artifacts, such as aliasing and incorrect wavefield reconstruction, ultimately leading to unreliable results.

Table 4 presents the count of bad shot records and traces that were either muted or interpolated during trace editing. In total, 4 out of 277 shot records were successfully interpolated, while 20 shot records could only be muted prior to the subsequent processing workflow.

Table 3. Processing tools and parameters used in trace editing.

Tool	Key Parameter	Value
Despike	Time window length (ms)	500.0
	Time window overlap (%)	25.0
	Number of traces in estimation window	21.0
	Trace window overlap (%)	25.0
	Averaging type	Mean
	Threshold multiple of median RMS	5.0
	Replacement scalar	1.0
	Interpolation type	Delaunay
Bandpass filter	Filter	6/50dB - 90/50dB
	Domain	Frequency
	Filter length	500.0
Trace edit (sht. sort)	Edit Mode	Zero trace
Fourier regularisation (sht. sort)	Time patch size (ms), overlap (%)	20.0, 25.0
	FFID patch size (# traces), overlap (%)	9, 25.0
	Tapering mode	Cos Before, Cos After
	Maximum gap (# traces)	5
	Convergence threshold (dB)	-40.0
	Maximum frequency (Hz)	125.0
Trace edit (chn. sort)	Edit Mode	Zero trace
Fourier regularisation (chn. sort)	Time patch size (ms), overlap (%)	20.0, 25.0
	channel patch size (# traces), overlap (%)	7, 25.0
	Tapering mode	Cos Before, Cos After
	Maximum gap (# traces)	3
	Convergence threshold (dB)	-40.0
	Maximum frequency (Hz)	125.0

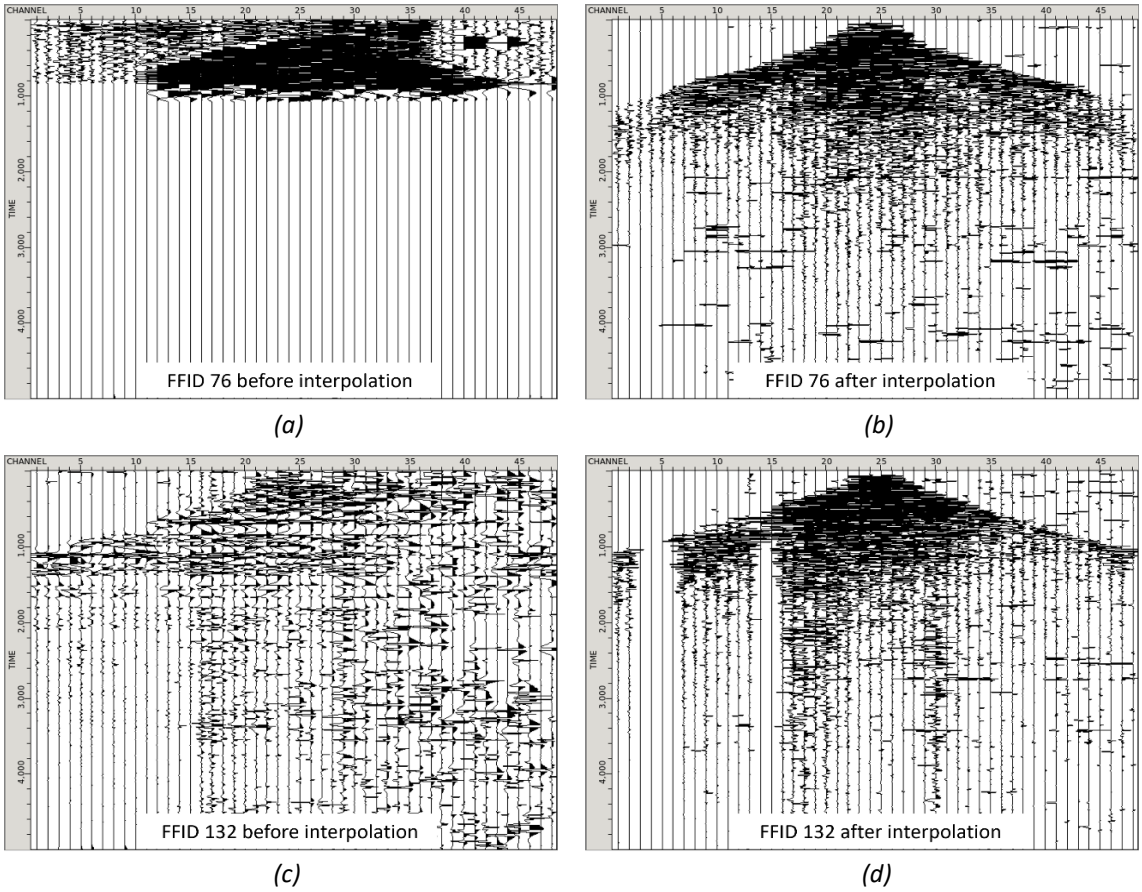

(a) *(b)*

(c) *(d)*

Figure 7. (a) and (b) show the shot record for FFID 76 before and after interpolation, respectively. (c) and (d) show the shot record for FFID 132 before and after interpolation, respectively.

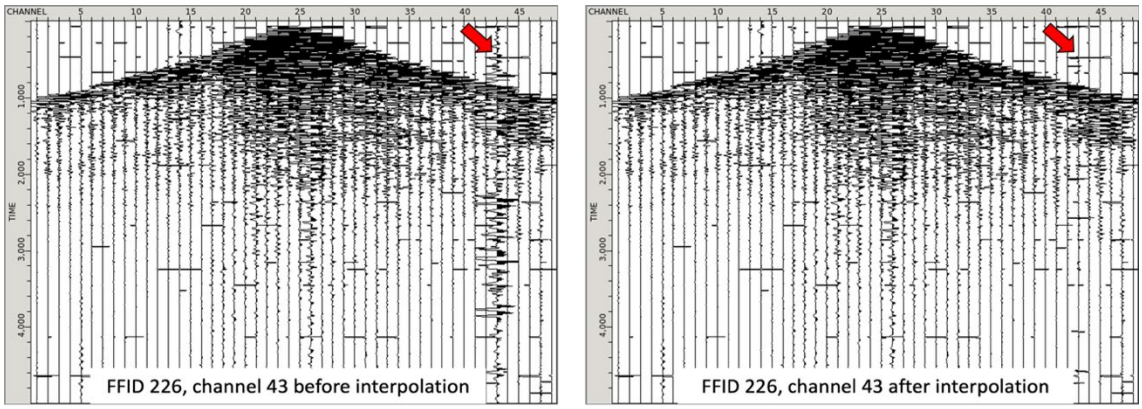

(a) *(b)*

Figure 8. (a) and (b) show a channel before and after interpolation, respectively. Red arrows highlight the differences.

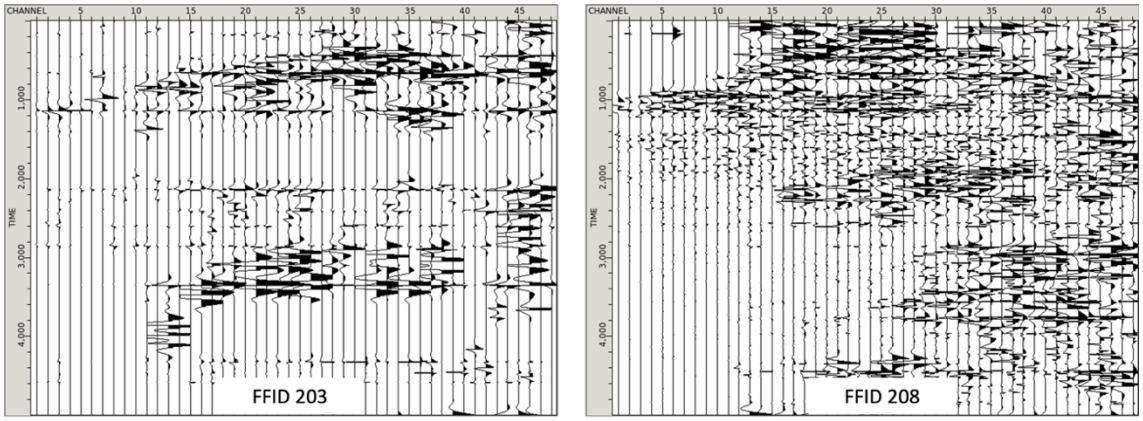

(a) *(b)*

Figure 9. Examples of shot gathers that could not be interpolated and were therefore muted in the subsequent processing workflow.

Table 4. Count of bad shot records and traces muted or interpolated during trace editing.

	Bad shot record	Bad trace	Total in trace
Input	24	31	1183
Interpolated	4	17	209
Muted	20	14	974

2.3 Static correction

This work utilized tomostatics, i.e., a static correction method that uses tomographic inversion of first-arrival travel times to estimate near-surface velocity variations and correct for time delays caused by shallow subsurface heterogeneities.

Tomostatics was performed using the following steps:

1. First-arrival travel-time picking

   First-arrival travel times were semi-automatically picked. The picks were then manually reviewed and edited, including repicking poorly interpolated arrivals, removing picks that deviated from the general trend in the offset sort, and eliminating picks with high reciprocal errors. Specifically, picks with reciprocal errors greater than approximately 22 ms were removed, as the majority of picks had reciprocal errors below this threshold.

2. Initial near-surface velocity model building

   An initial near-surface velocity model was constructed using the first-arrival travel-time picks. A uniform grid spacing of 5 meters was applied to define the model resolution. The resulting model is shown in Figure 10.

3. Ray tracing

   Ray tracing was used to calculate ray paths through the shallow subsurface. These ray paths connect the observed first-arrival travel times to the subsurface velocity structure

and guide the tomographic updates required to resolve near-surface velocities. Figure 11 shows the tomographic ray paths beneath the seismic line.

Several tomography runs were tested to achieve the best balance between model quality and the misfit between observed and inverted first-arrival travel times. The final result yielded a root-mean-square (RMS) misfit of 12.73 ms across all shots, with a maximum per-shot RMS misfit of 22.30 ms. Figure 13 shows the inverted near-surface velocity model beneath the seismic line, and Figure 12 presents an example of the fitting quality between observed and inverted first-arrival travel times for a single shot gather.

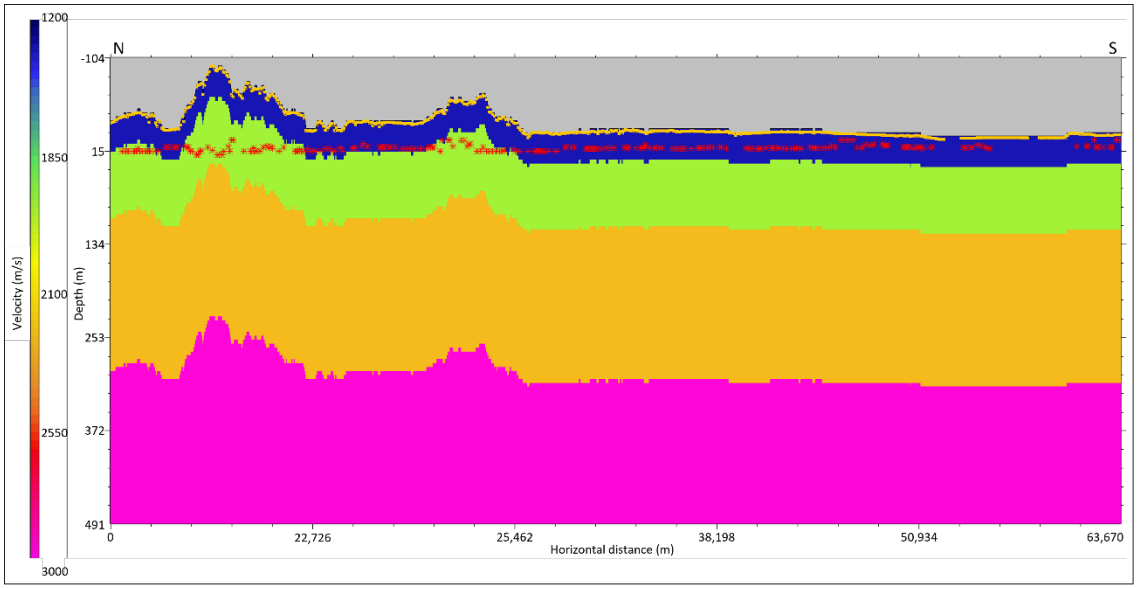

Figure 10. Initial near-surface velocity model used for tomographic inversion. Yellow and red asterisks represent receiver and source positions, respectively.

4. Performing static correction

   Before applying the static shifts, the static mean calculated using a 10-point smoothing window was removed. A replacement velocity of 2000 m/s was used for the correction.

5. Performing refraction residual static correction

   Model-based refraction residual static correction was applied in addition to the standard static correction, using minimum and maximum refraction offsets of 0 and 2400 meters, respectively.

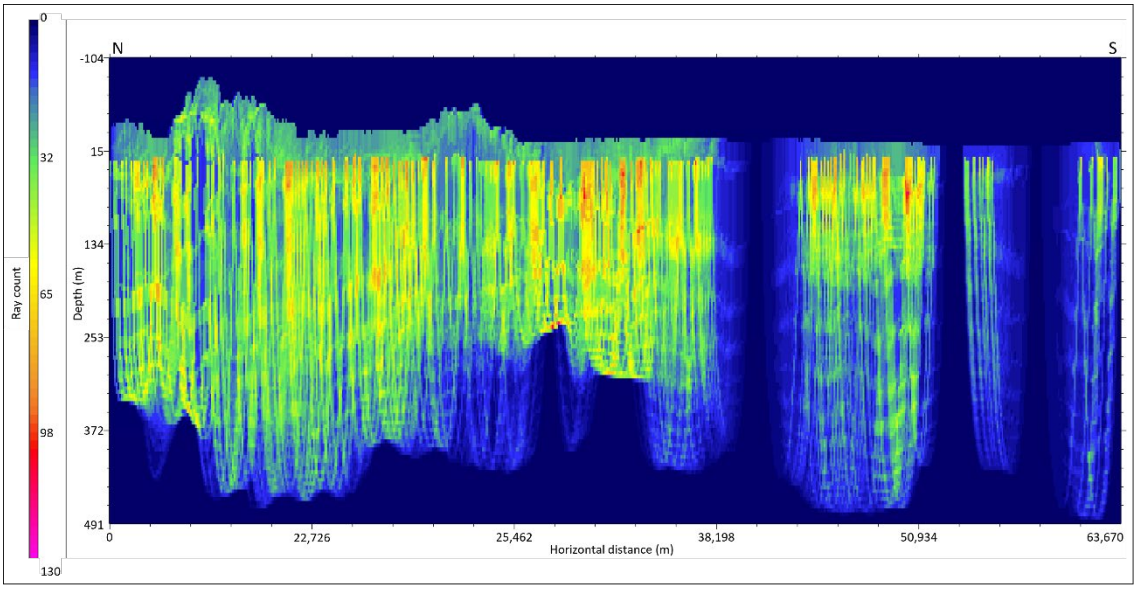

Figure 11. Tomographic ray paths beneath the seismic line.

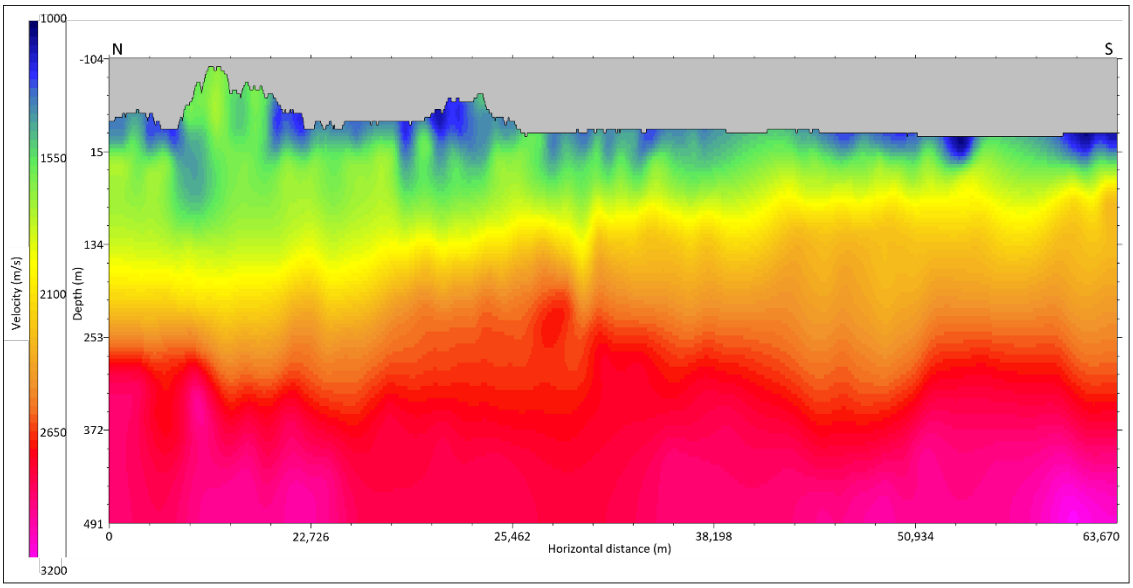

Figure 12. Inverted near-surface velocity model beneath the seismic line.

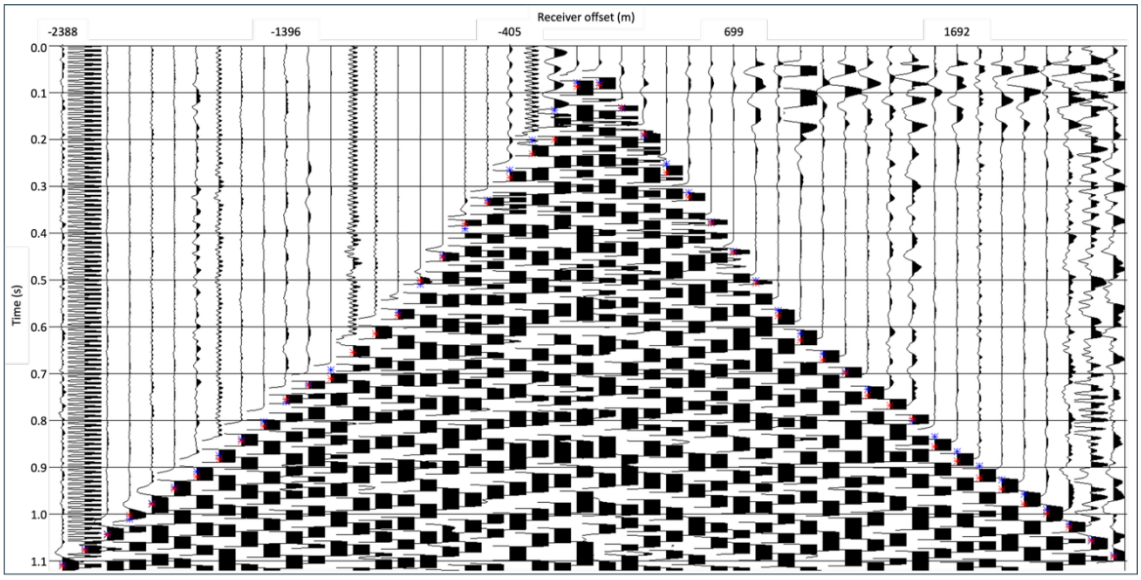

Figure 13. Comparison of observed (red asterisks) and inverted (blue asterisks) first-arrival travel times for a single shot gather, illustrating a relatively good fit between the two.

2.4 Preprocessing

Preprocessing was performed to produce NMO-corrected gathers, which were later used to calculate stack power static corrections. The stacking velocity table was derived from velocity

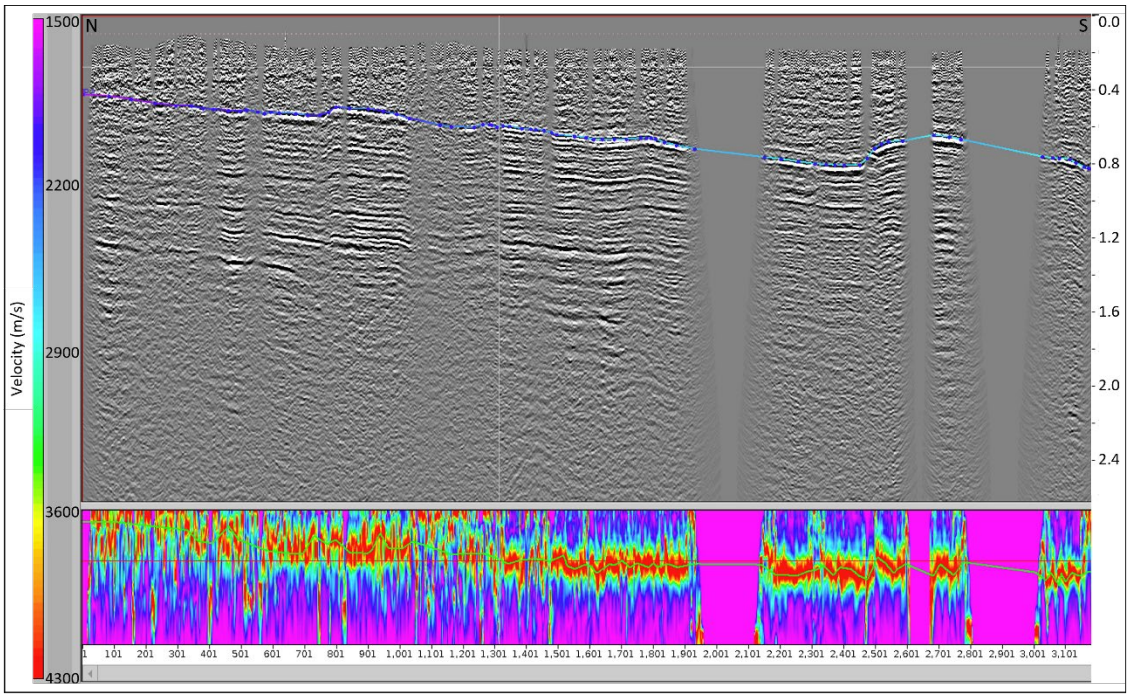

Figure 14. Velocity analysis panel based on a constant-velocity-stack (CVS) cube. The top panel displays a seismic stack generated using a stacking velocity of 2500 m/s. The bottom panel shows a semblance plot in the distance (X) and velocity (V) domain.

analysis using a constant-velocity-stack (CVS) cube. With this approach, stacking velocities were consistently picked along key seismic reflections or horizons. Figure 14 shows an example of a velocity analysis panel using a CVS cube from the reprocessing. Table 5 lists the processing tools and key parameters used during preprocessing.

Table 5. Processing tools and key parameters used in the preprocessing stage.

Tool	Key Parameter	Value
Top mute	Mode	First-break mute
	Added offset (m), time-shift (ms)	0,0; 3000, 300
Bandpass filter	Filter (Hz)	5-12-50-60
Deconvolution	Type	Predictive
	Prediction lag (ms)	36.0
	Operator length (ms)	100.0
Bandpass filter	Filter (Hz)	5-12-50-60
Trace balancing	Time window (ms)	0.0-5000.0
Static correction	Method	Tomostatics
	Replacement velocity (ms)	2000.0
	Remove mean statics (point)	10.0
Refraction residual static correction	Mode	Model-based
	Minimum refraction offset (m)	0.0
	Maximum refraction offset (m)	2400.0
Velocity analysis I (stacking velocity)	Method	CVS cube
	Replacement velocity (m/s)	2000.0
	Velocity range (m/s)	1500-5000
	Velocity interval (m/s)	25.0
	Shot range	1-277
	Shot increment	1.0
	Maximum offset (m)	2400
	Stretch limit (%)	20.0

2.5 Processing

The processing stage consists of the following three main steps:

1. Reflection residual static correction
2. Signal processing (signal-to-noise ratio enhancement)
3. Velocity analysis

These three steps were performed iteratively in two passes with practically the same key parameters. Table 6 shows processing tools in the processing stage and their key parameters.

Table 6. Processing tools and parameter keys used in the processing stage.

Tool	Key Parameter	Value
Stack power residual static correction I	Time window start (ms)	400.0
	Time window end (ms)	2000.0
	Maximum source/receiver shift (ms)	10.0
Time-offset scaling	Power of time	0.5
	Power of offset	0.0
Surface consistent deconvolution	Type	Predictive
	Prediction lag (ms)	36.0
	Operator length (ms)	100.0
Time-variant spectral whitening	Frequency range (Hz)	29434.0
	Frequency taper (Hz)	5.0
	Number of frequency bands	10.0
FX Cadzow filter	Signal frequency range (Hz)	5-12-55-70
	Number of eigenimages	2.0
	Local zone radius (m)	600.0
	Local zone azimuth range (degree)	360.0
	Local time window (ms)	300
Bandpass filter	Filter (Hz)	5-12-80-95
Velocity analysis II (stacking velocity)	Method	CVS cube
	Replacement velocity (m/s)	2000.0
	Velocity range (m/s)	1500-5000
	Velocity interval (m/s)	25.0
	Shot range	1-277
	Shot increment	1.0
	Maximum offset (m)	2400
	Stretch limit (%)	20.0
Stack power residual static correction II	Time window start (ms)	400.0
	Time window end (ms)	2000.0
	Maximum source/receiver shift (ms)	10.0

2.6 Migration

The seismic data were migrated using a post-stack time migration (POSTM) technique. This stage included obtaining a root-mean-square (RMS) velocity model for migration and applying post-migration processing. Before the migration, the data were clipped to a length of 4000 ms.

Table 7 lists the processing tools and key parameters applied during the migration stage, which marks the final step of the reprocessing workflow. Figure 15 presents the final reprocessing output.

Table 7. Processing tools and parameter keys used in the migration stage.

Tool	Key Parameter	Value
Velocity analysis III (RMS velocity)	Method	CVM cube
	Replacement velocity (m/s)	2000.0
	Migration frequency range (Hz)	5-95
	Velocity range (m/s)	1500.0-4250.0
	Velocity interval (m/s)	50.0
	Shot range	1-277
	Shot increment	1
	Migration aperture (m)	4000.0
	Maximum offset (m)	2400.0
	Number of offset sections	24
	Stretch limit (%)	10.0
	Mute angles (degree)	15.0
Post-stack time migration	Algorithm	Phase-shift time migration
	Velocity percentage (%)	5.0
	Maximum frequency (Hz)	95.0
	CMP spacing (m)	10.0
Structure-oriented denoise	CMP search increment	1.0
	Time search incerement (ms)	50.0
	Maximum search dip (ms/bin)	1.0
	CMP search radius (bins)	5.0
	Semblance search window (ms)	50.0
Bandpass filter	Filter (Hz)	8-15-90-110

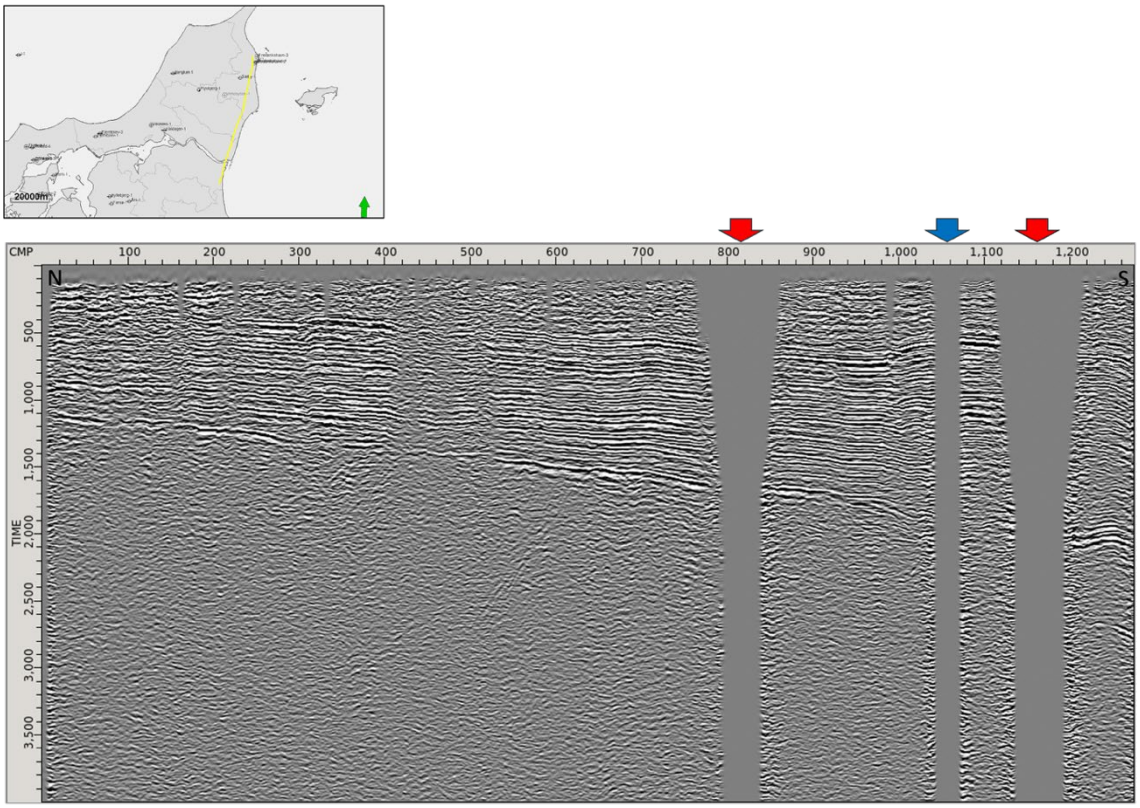

Figure 15. Final reprocessing result obtained using a post-stack time migration workflow. Red arrows indicate gaps in the seismic profile caused by missing input data for the reprocessing. Blue arrow marks the location of the Limfjord channel. Yellow line on the map shows the position of the seismic line. Green arrow on the map indicates north.

3. Comparison with the legacy seismic profile

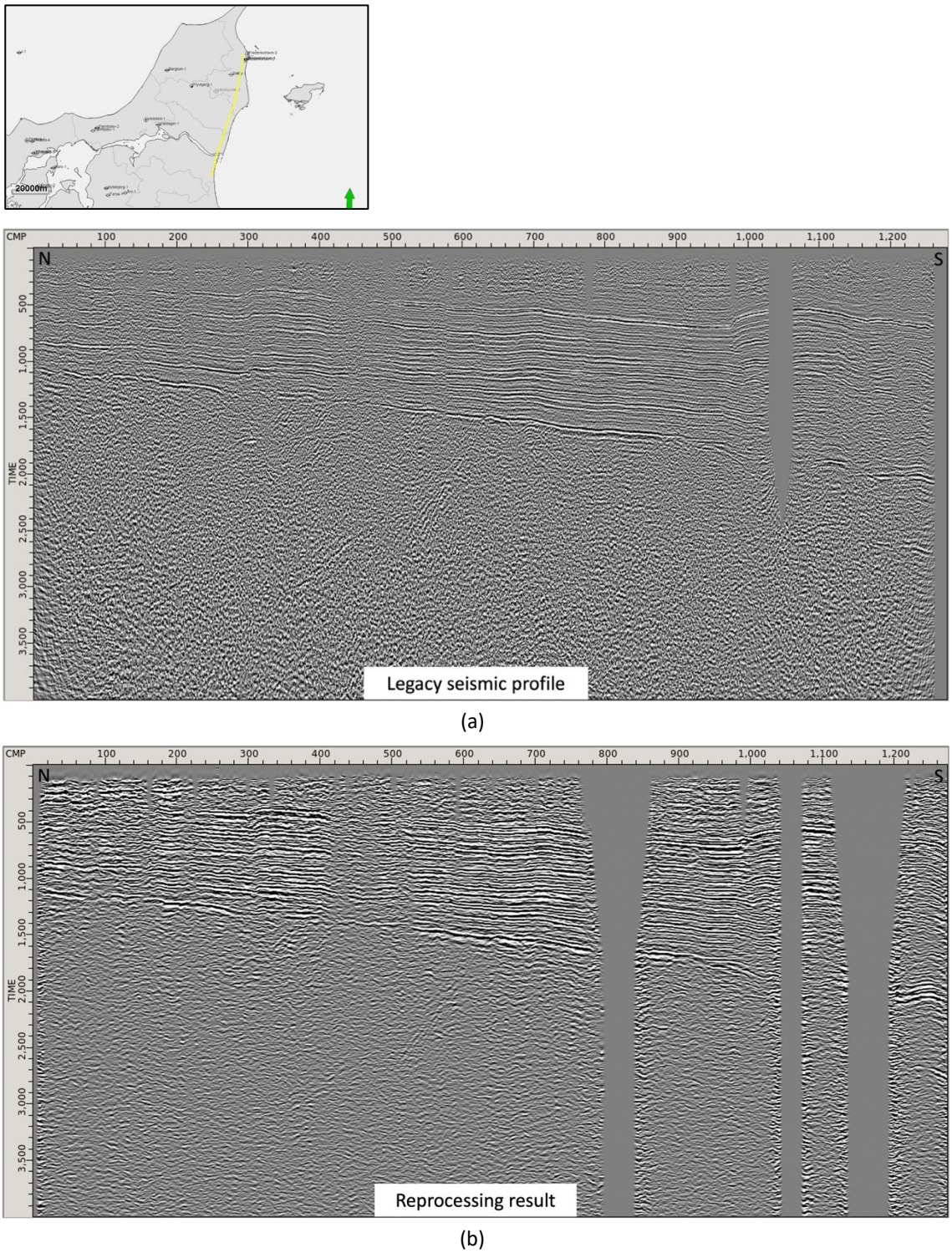

Figure 16. Comparison between (a) the legacy seismic profile and (b) the reprocessed result. The yellow line on the map shows the position of the seismic line. Green arrow on the map indicates north.

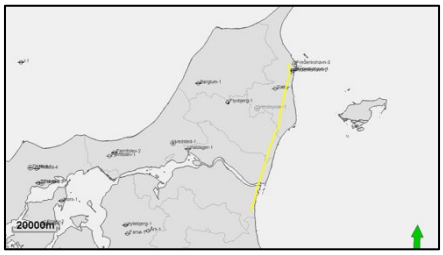

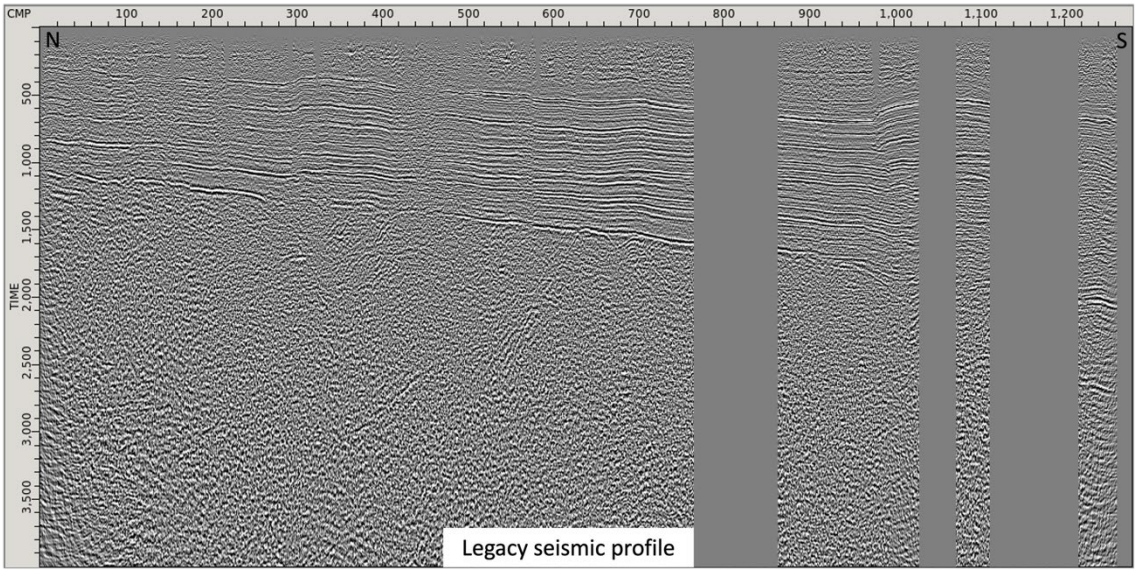

(a)

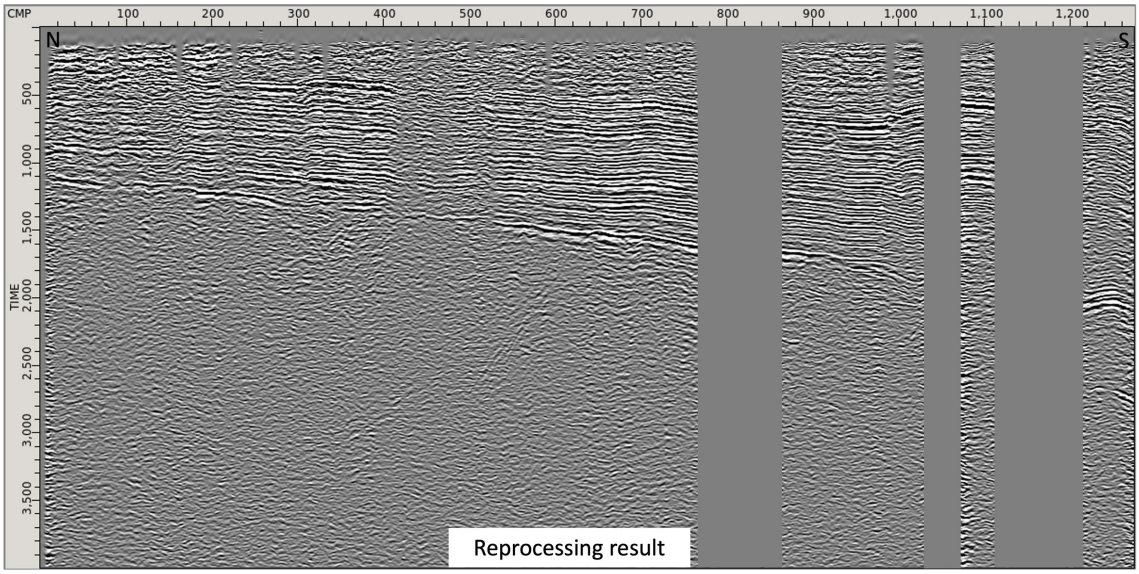

(b)

Figure 17. Comparison between (a) the legacy seismic profile and (b) the reprocessed result. The same parts of both profiles are masked to match the areas of missing data in the reprocessing result. Yellow line on the map indicates the location of the seismic survey line. Green arrow on the map indicates north.

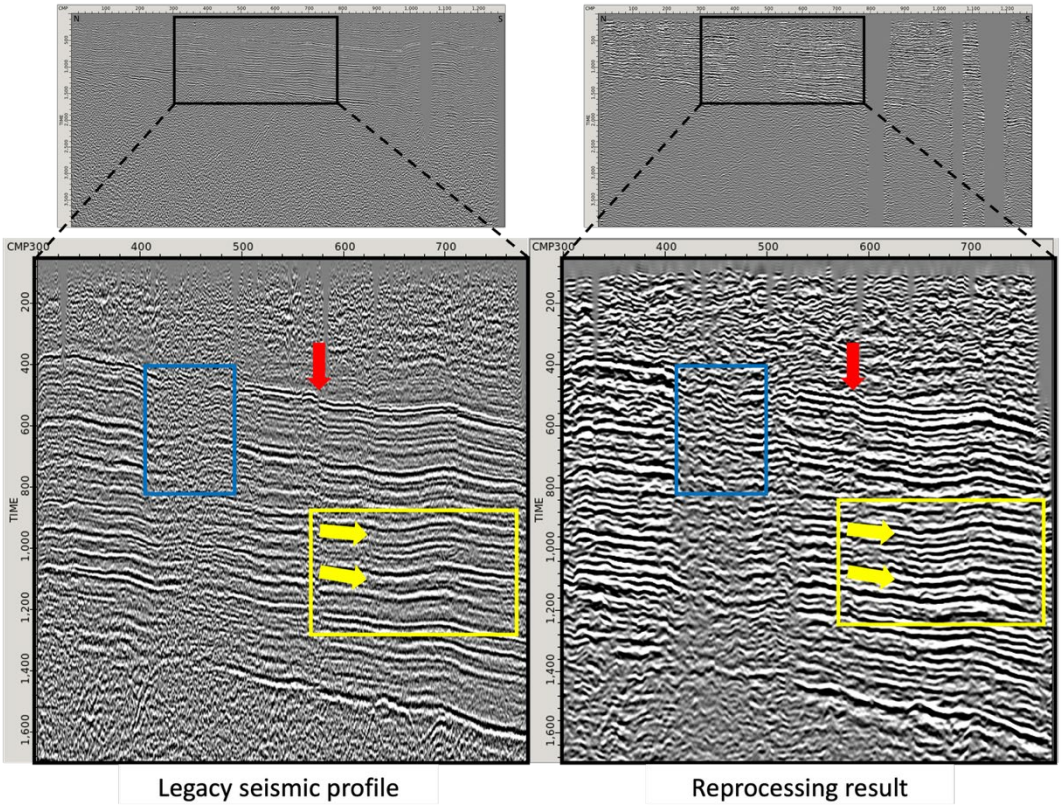

Figure 18. Close comparison between the legacy profile (left) and the reprocessing result (right). Yellow boxes highlight areas where differences between the two profiles are evident. Yellow arrows indicate high-resolution coherent reflections associated with thinner geological strata, which are not visible in the legacy profile. Blue boxes mark zones where the reprocessing result improves imaging in reflector-free regions of the legacy data. Red arrows point to a fault-like structure in the legacy profile that appears less pronounced in the reprocessing result. Arguably, this feature may also be interpreted as an artifact caused by low fold coverage at the corresponding common mid-point (CMP) location, as it appears perfectly vertical and coincides with a low-fold area indicated by near-surface characteristics of the profile.

4. Acknowledgment

We thank Anders Mathiesen for providing alternative source and receiver elevation data based on a topographic map, Ulrik Gregersen for sharing his insights on the geology of the area, Kenneth Nordstrøm for assisting in verifying the availability of navigation data, and Peter Voss for reviewing this report.